Dynamic scaling of roughness at the early stage of tungsten film growth

Luca Peverini and Eric Ziegler
European Synchrotron Radiation Facility, Boîte Postale 220, 38043 Grenoble Cedex, France

Thierry Bigault
Institute Laue-Langevin, Boîte Postale 156, 38042 Grenoble Cedex, France

Igor Kozhevnikov
Institute of Crystallography, Leninsky prospect 59, Moscow 119333, Russia

(Received 2 February 2007; revised manuscript received 22 May 2007; published 12 July 2007)

The roughening of sputter-deposited tungsten films is studied *in situ* and in real time using grazing incidence x-ray scattering. It is shown that the power spectral density functions characterizing the external film surface roughness and the film-substrate roughness conformity can be uniquely extracted from a single scattering diagram when measured at a grazing incidence angle exceeding the critical angle of total external reflection. The temporal evolution of the roughness spectrum is demonstrated to obey a universal scaling form leading to a roughness exponent $\alpha=0.18\pm0.02$ and to an extremely small growth exponent $\beta=0.06\pm0.01$. In accordance with the scaling theory, these values of the scaling exponents provide a collapse into a single master curve of the "renormalized" power spectral density functions for film thicknesses ranging between 2 and 25 nm.

DOI: 10.1103/PhysRevB.76.045411 PACS number(s): 78.70.Ck, 68.35.Ct, 75.40.Gb

Sputter deposition of thin films is the foundation of many surface processing techniques, including deposition of layered structures in multilayer coated optics, giant-magnetoresistance thin films, and layered devices in microelectronics. In all these applications, the presence of surface roughness typically results in the scattering of light or electrons and therefore in a "loss" of energy and of coherence. For these reasons, it is still a challenging task in technology to characterize quantitatively the surface roughness evolution of thin films and, on this basis, to establish the optimal growth process conditions resulting in the smoothest film possible. A widely accepted theoretical scheme is to describe the thin film growth dynamics under the concept of dynamic scaling.[1–3] Here, the surface roughness $\sigma(t)$ of a film growing under nonequilibrium conditions on an ideally smooth substrate increases with time t as a power law $\sigma(t)\sim t^{\beta}$ as long as the correlation length $\xi(t)\sim t^{1/z}$ is smaller than the system size L. Further growth does not change the surface topography of the film, with the saturated roughness depending on the system size $\sigma_{sat}\sim L^{\alpha}$. Following this concept, several attributes α, β, and $z=\alpha/\beta$, known as scaling exponents, can be used as the signatures in space and time of highly complex film growth processes. By comparing the experimental scaling exponents with the theoretical predictions, one can recognize the type of differential equation describing the film growth and, hence, classify a growth process within a certain universality class.[2] However, although very thin films are of great technological interest, the experimental determination and verification of the scaling approach in this regime and in the case of sputter deposition are still lacking. Some works found in literature have provided evidence that, in the case of sputter deposition of films with thickness greater than 100 nm, roughness is evolving with time following a scaling law.[4–6] Nevertheless, these grounds do not provide a full quantitative assessment of the phenomena at the initial stage of growth.

In this paper, we study *in situ* the temporal evolution of roughness of sputter-deposited tungsten films at the initial stage of growth, i.e., for film thicknesses ranging between 2 and 25 nm using grazing incidence x-ray scattering (XRS). We demonstrate an unusual variation in the surface topography with film thickness marked by an extremely small growth exponent $\beta\approx0.06$. As a result, the root-mean-squared (rms) roughness is increased from 0.13 nm for the initial silicon substrate up to only 0.2 nm after the growth of a 25 nm thick tungsten film. Such a small growth exponent does not correspond to any growth equation analyzed in literature and until now was only observed in molecular beam epitaxy deposition.[2] In addition, we justify the validity of the Family-Viscek scaling hypothesis at the initial stage of film growth through the demonstration of collapse into a single curve of the "renormalized" power spectral density (PSD) functions measured at various film thicknesses through proper choice of the scaling exponents. The interest on studying tungsten film growth in this range of film thickness is mainly due to the wide use of short-period tungsten-based multilayer mirrors in x-ray optical systems.

In our experiment, the scattering diagrams were integrated over the azimuth scattering angle by collecting a rather large (5 mm) part of the incident beam in the direction perpendicular to propagation, thus allowing us to increase the scattered radiation intensity and to decrease the measuring time. In the frame of the first-order scalar perturbation theory, the integrated scattering diagram from an isotropic film reads

$$\Pi(\theta,h)=\frac{1}{W_{inc}}\frac{dW_{scatt}}{d\theta}=\frac{k^3}{16\pi\sin\theta_0}[A_f\mathrm{PSD}_{ff}(p,h)+A_s\mathrm{PSD}_{ss}(p)+A_{sf}\mathrm{PSD}_{sf}(p,h)],$$

$$k=\frac{2\pi}{\lambda},\quad p=\frac{1}{\lambda}|\cos\theta-\cos\theta_0|, \tag{1}$$

 ©2007 The American Physical Society

where W_{inc} and dW_{scat} are the radiation powers of the incoming beam impinging under an angle θ_0 and of the beam scattered within an angular interval $d\theta$ under an angle θ with respect to the sample surface. The electrodynamics factors A_j contained in Eq. (1) do not depend on the thin film roughness and have the following form:

$$A_f = |(1-\varepsilon_f)[1+r(\theta_0,h)][1+r(\theta,h)]|^2,$$

$$A_s = |(\varepsilon_f-\varepsilon_s)t(\theta_0,h)t(\theta,h)|^2,$$

$$A_{sf} = 2\,\mathrm{Re}\{(1-\varepsilon_f)(\varepsilon_f-\varepsilon_s)^*[1+r(\theta_0,h)] \times[1+r(\theta,h)]t^*(\theta_0,h)t^*(\theta,h)\},$$

where ε_s and ε_f are the dielectric constants of the substrate and of the film, and $r(\theta,h)$ and $t(\theta,h)$ are the amplitude reflectance and transmittance of a perfectly smooth film of thickness h.

The scattering properties of a rough film are thus characterized entirely by three one-dimensional (1D) PSD functions, $\mathrm{PSD}_{ss}(p)$ and $\mathrm{PSD}_{ff}(p,h)$, describing the roughness of the substrate and of the external film surface, and $\mathrm{PSD}_{sf}(p,h)$, determining the statistical correlation (conformity) between film and substrate roughnesses: $\mathrm{PSD}_{ij}(p) = 4\int\langle\zeta_i(\vec{\rho})\zeta_j(0)\rangle\cos(p\rho)d\rho$ with $i,j=\{s,f\}$ and where the stochastic functions $\zeta_s(\vec{\rho})$ and $\zeta_f(\vec{\rho})$ describe the substrate and the film relief, respectively. The angular brackets denote an ensemble averaging and p is the spatial frequency.

In expression (1), the first two terms describe the intensity scattered from the film surface and from the substrate, while the third one results from the interference of the waves scattered by the various interfaces having conformal roughness.[7] By measuring the scattering diagram at different angles θ_0 or different radiation wavelengths λ, one can use Eq. (1) to form a system of linear algebraic equations dependent on $\mathrm{PSD}_{ff}(p)$ and $\mathrm{PSD}_{sf}(p)$, provided the function $\mathrm{PSD}_{ss}(p)$ of the substrate remains unchanged during deposition. For each value of the spatial frequency p, the unknown PSD functions can then be found without using any model of correlation function. Since two unknown functions need to be determined, such an analysis normally requires, at least, two different sets of scattering data obtained either at different grazing angles or at different x-ray energies. This approach was successfully demonstrated, e.g., in our recent work,[8] where we recorded two sequences of XRS diagrams during two growth experiments although that might introduce manifold artifacts. A more accurate approach consists of measuring XRS diagrams from the same growing film at two incidence angles or x-ray energies simultaneously. However, this approach would require a sophisticated setup capable of quickly switching from one tuning position to the other at any moment during growth. Below, we will analyze a way of overcoming these difficulties and will demonstrate that two unknown PSD functions can be uniquely extracted from a single XRS diagram, thanks to a peculiar feature of Eq. (1).

If the grazing angle θ_0 of the probe beam exceeds the critical angle of total external reflection (TER), the coefficient A_{sf} (an oscillating function of the scattering angle θ) is responsible for the appearance of oscillations in the XRS diagram. An experimental example is presented in Fig. 1. Here, a selection of scattering diagrams from the tungsten film measured at 5 s time intervals is shown.

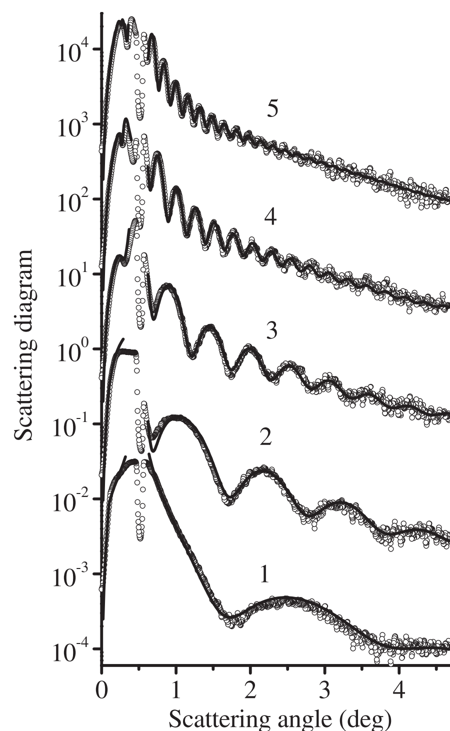

FIG. 1. XRS diagrams (circles) measured *in situ* and in real time at progressive tungsten film thickness: (1) 1.90 nm, (2) 3.83 nm, (3) 7.55 nm, (4) 15.75 nm, and (5) 24.6 nm. The data (except curve 1) are shifted vertically by factors of 30 for clarity. The solid curves were calculated using the PSD functions extracted from the experimental data.

Thin film deposition and XRS measurements were obtained under experimental conditions analogous to those indicated in Ref. 8: a superpolished silicon substrate flattened to $\lambda/10$ ($\lambda=632.8$ nm) has been processed and a W layer has been progressively grown onto it by magnetron sputtering. The experiment was performed at room temperature and the sputter time was adjusted to reach a final thickness of about 25 nm. Before process, the background pressure in the sputter chamber was less than 3.6×10^{-7} hPa. Then, magnetron sputtering was conducted in pure (99.999%) Ar gas at a working pressure of 1.33×10^{-3} hPa. The film growth was realized using a bias voltage of 370 V and a total target current of 30 mA, leading to a growth rate of 12.3 pm/s. The pressure set point was achieved by fixing the gas flow rate at a value of 3 SCCM (SCCM denotes cubic centimeter per minute at STP).

The x-ray measurements were performed setting the energy to 17.5 keV with a double-crystal Si (111) monochromator. The divergence in the vertical direction was 3×10^{-6} rad and the spectral purity $\Delta E/E$ of the order of 10^{-4}. The beam incidence angle with respect to the substrate surface was fixed and equal to 0.5°, i.e., about twice the critical angle of TER for bulk tungsten. The sharp minimum observed on each curve at the position of the specular peak is due to the presence of the beamstop placed in front of the

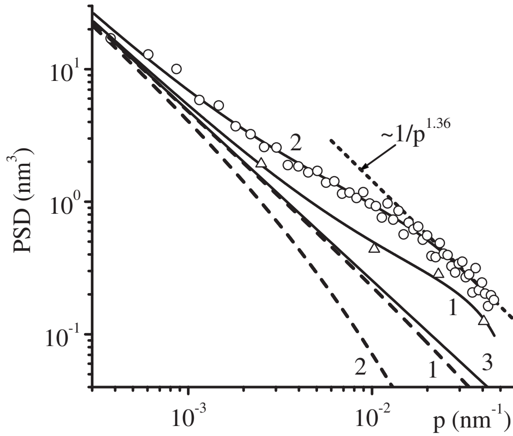

FIG. 2. The functions PSD_{ff} and PSD_{sf} (solid and dashed lines, respectively) of the (1) thinnest and (2) thickest films grown. The symbols represent the function PSD_{ff} extracted from XRS diagram directly. Curve 3 shows the PSD function of the substrate.

charge coupled device detector to prevent it from saturation. The reflectivity variation as a function of the deposition time, recorded at the same time as the XRS diagrams, was analyzed to infer the tungsten deposition rate (12.3 pm/s) and the film density ($18\ \mathrm{g/cm^3}$).

Figure 1 allows us to make a number of qualitative conclusions. First, the amplitude of the oscillations decreases with increasing scattering angle. Hence, the roughness conformity, i.e., the function PSD_{sf} determining the amplitude of these oscillations, decreases with increasing spatial frequency. Second, the roughness conformity decreases with increasing film thickness. For the thickest film (curve 5), the oscillations disappear at a scattering angle $\theta > 2.5°$, i.e., at $p > 13\ \mu\mathrm{m}^{-1}$, while they are still observed for thin films (curves 1 and 2). The coefficient A_{sf} is equal to zero at particular scattering angles θ, i.e., at particular spatial frequencies p. At these specific frequencies, we can find the PSD function of the external film surface PSD_{ff} directly from Eq. (1) assuming that the PSD function of the substrate PSD_{ss} is measured before deposition (Fig. 2, curve 3) and the substrate roughness does not change during film growth. The values obtained for PSD_{ff} are shown in Fig. 2 (symbols) for the thinnest (h=1.9 nm) and the thickest (h=24.6 nm) tungsten films. Evidently, the thicker the film, the higher the frequency of the oscillations of the coefficient A_{sf} and, hence, the greater the number of zeros of A_{sf} within the measurable range of the scattering angle (50 for the thickest film and only 4 for the thinnest one). Nevertheless, the behavior of the function $PSD_{ff}(p)$ is well established even for the thinnest film, because from general physical considerations we expect $PSD_{ff}(p)$ to be a smooth function of the spatial frequency. To decrease the statistical errors and to interpolate the PSD function between measured points, we represented the function $PSD_{ff}(p)$ in the following manner:

$$PSD_{ff}(p) = PSD_{ss}(p)\left(1 + \sum_{j=1}^{j_{\max}} a_j p^j\right), \qquad (2)$$

where typically $j_{\max}=3$. In addition, representation (2) implies a reasonable physical assumption of the roughness conformity at small spatial frequencies, i.e., $PSD_{ff}(p) \to PSD_{ss}(p)$ at $p \to 0$, allowing us to extrapolate the PSD function at low spatial frequencies. Such an analytic continuation is important especially for very thin films, when the number of zeros of the coefficient A_{sf} is little inside the measurable range of spatial frequency. The results of interpolation are presented in Fig. 2 (solid curves 1 and 2) for the thinnest and the thickest films. The PSD functions at intermediate thickness lie between these two extreme cases.

Once the PSD function of the external film surface is found, we can deduce the function $PSD_{sf}(p)$ as well using Eq. (2), the coefficients a_j being derived by fitting the calculated scattering diagram to the measured one. The PSD_{sf} functions obtained, which depict the roughness conformity, are shown in Fig. 2 (dashed curves 1 and 2) for the thinnest and the thickest films. Again, the intermediate PSD functions lie between these two curves. As one can see, the roughness conformity decreases exponentially with both film thickness and spatial frequency. The scattering diagrams calculated with the PSD functions found are in excellent agreement with the experimental data (Fig. 1, solid curves).

From a mathematical point of view, Eq. (1) considered as a system of linear equations for the unknown functions PSD_{ff} and PSD_{sf} should be analyzed separately with two sets of spatial frequency values. The first denumerable set $\{P_0\}$ comprises the spatial frequencies for which the coefficient $A_{sf}=0$. Then, the only unknown in Eq. (1) is the function $PSD_{ff}(p)$, whose values are found uniquely at the set $\{P_0\}$. Assuming $PSD_{ff}(p)$ to be a smooth function we can interpolate it, using Eq. (2), over the whole range of the measurable spatial frequency. Notice that, strictly speaking, the function $PSD_{sf}(p)$ cannot be found at the set $\{P_0\}$. The second continuous set of spatial frequencies contains all spatial frequencies excluding the set $\{P_0\}$. Here, system (1) contains both $PSD_{ff}(p)$ and $PSD_{sf}(p)$ as unknown functions. Since the function $PSD_{ff}(p)$ was interpolated over the whole range of spatial frequency, we can now extract $PSD_{sf}(p)$ from the same scattering diagram [from Eq. (1) at the same θ_0 and λ] except, strictly speaking, at the set $\{P_0\}$. To regularize the determination of the PSD functions, a typical ill-conditioned problem, we use interpolation (2).

The PSD functions provide a rather comprehensive description of the film roughness and allow us to calculate the various statistical parameters characterizing a growth process. In accordance with the Family-Viscek theory,[1,2] the 1D PSD function obeys the scaling relation, which can be written in the following form: $PSD_{ff}(p,h) \sim p^{-1-2\alpha} g(p^{1+2\alpha} h^{(1+2\alpha)/z})$, where the scaling function $g(u) \sim u$ for $u \to 0$ and $g(u) \to$ constant for $u \to \infty$. Hence, by plotting the renormalized function $PSD_{ff}(p,h)p^{1+2\alpha}$ versus the renormalized spatial frequency $p^{1+2\alpha}h^{(1+2\alpha)/z}$ at different film thicknesses h and with a proper choice of the scaling exponents α and z, it is possible to obtain the collapse of all curves into a single master curve corresponding to the scaling function $g(u)$. Figure 3 illustrates this effect. The graph was drawn using eight PSD functions determined from the scattering diagrams measured at eight different film thickness from 1.9 to 24.6 nm. The data collapse was clearly observed for a roughness exponent α =0.18 and a dynamic

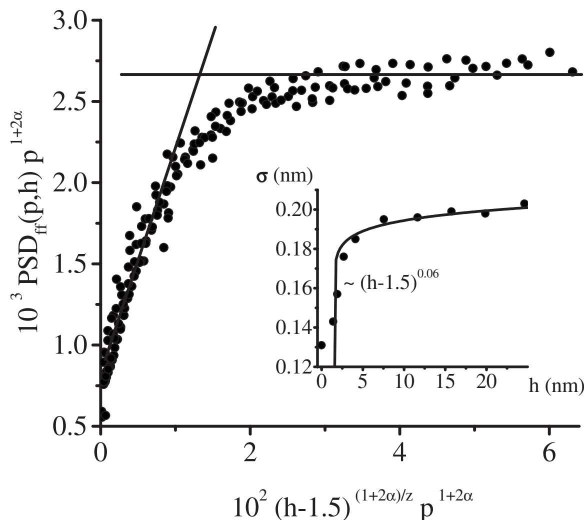

FIG. 3. Illustration of the data collapse obtained with eight PSD functions representing the external tungsten film surface for layer thickness ranging from 1.9 to 24.6 nm. Inset: Thickness dependence of the rms roughness of the external film surface superimposed to a power law with growth exponent $\beta=\alpha/z=0.06$.

exponent $z=3$. The error on the determination of these values was estimated to be about ±10%. The straight solid lines indicate the asymptotic behavior of the scaling function at small and large argument values. The dispersion of the experimental points in Fig. 3 probably originates from the inaccuracy on the determination of the PSD functions.

We would like to emphasize the following features of the data collapse observed. First, the experimental scaling function $g(u)$ tends to a nonzero value when decreasing the argument u. We believe that it is due to the substrate roughness. The classical formulation of the scaling model assumes a perfectly smooth substrate or, at least, very smooth as compared to that of the film surface. Here, the rms roughness of the deposited W film (about 0.2 nm at the higher thickness) is comparable to that of the substrate (0.13 nm). Second, to observe the data collapse at very low film thickness, of the order of 2–4 nm, we had to replace the nominal thickness h by an effective one $h'=h-1.5$ nm. It is conceivable that the scaling exponents we found could only describe the growth dynamics of the film after a certain thickness, e.g., once it gets continuous. The film formed during the initial stage of growth (nominal thickness <1.5 nm), possibly discontinuous, might obey, if at all, another scaling law. Obviously, a justification of this statement calls for additional experiments. Third, the scaling exponents derived correspond to none of the growth exponents reported in the literature. Notice that such disagreement between experimental scaling exponents and theoretical predictions has already been pointed out by other authors[4,9] and may be due to the high degree of complexity of the film growth dynamics. Therefore, a more comprehensive theory should take into account the following contributions: (a) The first is the effect of the substrate roughness on the film growth. As it was demonstrated in Ref. 10, the coarsening exponent $1/z$ depends on both the height distribution and the correlation function of the substrate roughness. (b) The second is the gradual crystallization of tungsten with progressive thickness. The influence of this factor on the growth dynamic was discussed in Ref. 9. (c) The third is the fact that the sputter deposition, involving several processes including implantation and interdiffusion of tungsten atoms into silicon substrate, may lead to a change of the substrate roughness and of the dielectric constant profile, and hence, to a less rigorous treatment. However, our first experimental study of the substrate roughness variation during tungsten film growth[11] demonstrated that intermixing occurring at the film—substrate interface does not change appreciably the substrate roughness, at least in the measurable range of the spatial frequencies $p<0.05$ nm^{-1}. Nevertheless, a complete study would require a full understanding of all phenomena listed above and the carrying out of a set of dedicated experiments. In this sense, our work should be considered as a step of a large subject of research.

The asymptotic behavior of the PSD function of the thickest film at high spatial frequency (see Fig. 2, dotted curve) corresponds to an inverse power law $p^{-(1+2\alpha)}$ with a roughness exponent $\alpha=0.18$, the same as that found from the data collapse. The inset in Fig. 3 shows the dependence of the rms roughness on the film thickness obtained by integration of the PSD function over the measurable range of spatial frequency $p\in[3\times10^{-4},4.6\times10^{-2}\ \text{nm}^{-1}]$. As above, we replaced the nominal film thickness h by an effective one $h'=h-1.5$ nm. The solid curve is in accordance with the scaling model assuming a power-law dependence of the rms roughness on the film thickness $\sigma\sim h^{\beta}$. The small value of the growth exponent $\beta=\alpha/z=0.06$ expresses the very slow increase of rms roughness with film thickness. We would like to recall that the same growth exponent was determined from the data collapse. Such a small rise of the roughness value is often observed at the early stage of growth of sputter-coated films. Just this property explains the extensive application of the sputtering technique to grow very smooth films, e.g., short-period multilayer interferential mirrors.[12] However, this slow increase of roughness is only observed when the W film is truly thin, i.e., for thicknesses less than 25–30 nm. Further film growth results in a dramatic development of roughness. A roughness of 2.5 nm was measured for a 70 nm thick film, probably due to the crystallization of tungsten. The evolution of roughness in this growth regime obeys another law that will not be analyzed in the present paper, as the perturbation theory we used is invalid for too rough surfaces.

The scaling exponents extracted from the PSD functions of the external film surface $\text{PSD}_{ff}(p,h)$ characterize the general law describing the development of intrinsic film roughness. However, the optical properties of a rough film also depend on the conformity between film and substrate roughnesses (vertical correlation). To characterize it quantitatively, let us introduce, following Ref. 8, the replication factor

$$K(p,h)=\frac{\text{PSD}_{sf}(p,h)}{\sqrt{\text{PSD}_{ff}(p,h)\text{PSD}_{ss}(p)}}.$$

This factor, illustrated in Fig. 4, shows a quick decrease of the roughness conformity with increasing spatial frequency.

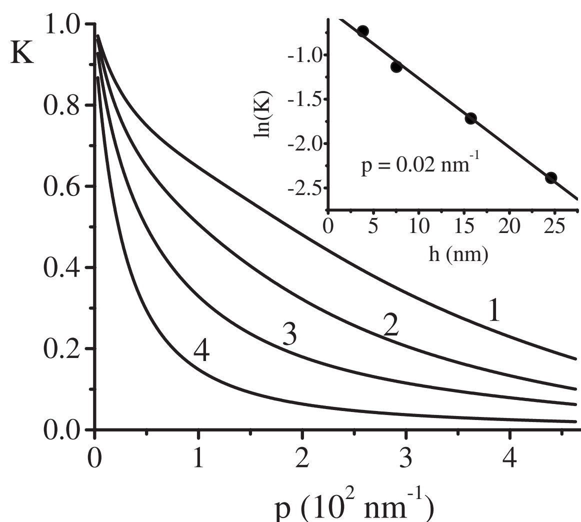

FIG. 4. Replication factor versus spatial frequency for different thicknesses of tungsten film: h are (1) 3.83 nm, (2) 7.55 nm, (3) 15.75 nm, and (4) 24.6 nm. Inset: Replication factor versus film thickness at the fixed spatial frequency $p=0.02\ \mathrm{nm}^{-1}$.

The inset in Fig. 4 shows an exponential decay of the vertical correlation with increasing film thickness.

In conclusion, we demonstrated that an XRS diagram measured at a single grazing angle exceeding the critical angle of TER and obtained *in situ* during thin film growth is sufficient to determine uniquely (a) the two PSD functions, $\mathrm{PSD}_{ff}(p,h)$ and $\mathrm{PSD}_{sf}(p,h)$, characterizing the statistical properties of the roughness of a film as a function of its thickness, (b) the scaling exponents characterizing the film growth dynamic, and (c) the vertical correlation (conformity) between the roughness of the film and of the substrate. We found that the growth of a tungsten film on a Si substrate in the thickness range from 1.9 to 25 nm complies with scaling laws, the scaling exponents being equal to $\alpha=0.18\pm0.02$ and $\beta=0.06\pm0.01$. The approach developed has a relevant technological impact because it can be applied *in situ* under various surface treatments (examples include deposition, ion etching, and oxidation).

One of the authors (I.K.) was supported by the ISTC (Project No. 2297).

[1] F. Family and T. Viscek, J. Phys. A **18**, L75 (1985).
[2] A.-L. Barabasi and H. E. Stanley, *Fractal Concepts in Surface Growth* (Cambridge University Press, Cambridge, 1995).
[3] P. Meakin, *Fractals, Scaling and Growth Far from Equilibrium* (Cambridge University Press, Cambridge, 1998).
[4] J. Krim and G. Palasantzas, Int. J. Mod. Phys. B **9**, 599 (1995).
[5] B. Q. Li, I. Kojima, and J. M. Zuo, J. Appl. Phys. **91**, 4082 (2002).
[6] M. A. Auger, L. Vazquez, R. Cuerno, M. Castro, M. Jergel, and O. Sanchez, Phys. Rev. B **73**, 045436 (2006).
[7] A. Yu. Karabekov and I. V. Kozhevnikov, Proc. SPIE **2453**, 176 (1995).
[8] L. Peverini, E. Ziegler, T. Bigault, and I. Kozhevnikov, Phys. Rev. B **72**, 045445 (2005).
[9] M. Kardar, Physica B **221**, 60 (1996).
[10] C. Tang, S. Alexander, and R. Bruinsma, Phys. Rev. Lett. **64**, 772 (1990).
[11] E. Ziegler, L. Peverini, and I. Kozhevnikov, Abstracts of the Eighth International Conference on the Physics of X-Ray Multilayer Structures, Sapporo, March 2006 (unpublished), p. 51.
[12] E. Spiller, *Soft X-ray Optics* (SPIE Optical Engineering, Bellingham, WA, 1994).